Characterization of the secondary neutron field generated by a compact PET cyclotron with MCNP6 and experimental measurements

D. Alloni[1,2] and M. Prata[1,2]

[1] LENA, Laboratory of Applied Nuclear Energy, Cyclotron Laboratory, University of Pavia, Italy.
[2]INFN, National Institute of Nuclear Physics, Pavia Unit, Italy.
Corresponding author: daniele.alloni@unipv.it

Abstract. *The production of the most common used PET radioisotope Fluorine-18 with commercial cyclotrons is obtained from the $^{18}O(p,n)^{18}F$ nuclear reaction when ^{18}O-enriched water is bombarded with a proton beam. We present the characterization of the secondary neutron field spectra produced by this reaction in different locations around the cyclotron, through a comparison between MCNP6 Monte Carlo simulation results and experimental data obtained with Neutron Activation Analysis (NAA) of thin target foils of different materials.*

1 Introduction

- PET (Positron Emission Tomography) has become a widely used functional imaging technique for determining biochemical and physiological processes in vivo by using radiopharmaceuticals labeled with positron-emitting radionuclides such as ^{11}C, ^{13}N, ^{15}O and ^{18}F, mostly produced by commercial cyclotrons directly produced at health centers or at least nearby.
- During isotopes productions, an undesirable neutron field is however generated making, neutrons the main shielding problem to deal with. Furthermore, health physics program requires to determine the neutron energy spectrum as more detailed as possible, although neutron spectrum measurement is not a trivial task.
- One of the most commonly used radiopharmaceuticals is 2-deoxy-2-[^{18}F]fluoro-D-glucose ([^{18}F] FDG), which is labelled with the radioactive ^{18}F isotope obtained from the $^{18}O(p,n)^{18}F$ nuclear reaction when ^{18}O-enriched water is bombarded with a proton beam. As a product of this reaction, a secondary neutron field is formed in addition to the gamma rays generated upon de-excitation of the nuclides formed during ^{18}F production as well as in neutron-induced nuclear reactions occurring in the various cyclotron components and, in minor concentrations, in the bunker wall materials.
- In this work (Alloni and Prata, 2017), we study with the MCNP6 Monte Carlo N-Particle Transport Code (Goorley, 2012; Briesmeister, 2000) the secondary neutron field spectra in three different locations around a commercial cyclotron using detailed cyclotron and target geometrical models and compare the simulation results with experimental data obtained by means of Neutron Activation Analysis (NAA).

2. Materials and methods

2.1 Facility description and cyclotron/target modeling

- The device employed at the Laboratory of Applied Nuclear Energy (LENA) of the University of Pavia, is an **IBA cyclotron (model Cyclone® 18/9)** set up for 18 MeV proton bombardment of a highly ^{18}O-enriched H_2O (^{18}O>98.0 Atom %, provided by Huayi Isotopes Co.) target with a nominal 30 μA beam current **(Figure 1)**.
- To perform the simulations of neutron transport inside the bunker and to modelling the entire cyclotron geometry, the Monte Carlo MCNP6 code was used. **Figures 2, 3 and 4** show both a top and side views of the modeled cyclotron. The neutron flux positions where the neutron spectra have been tallied with MC calculations are indicated by circles with cross symbols. At the same locations, NAA measurements with target foils have been carried out.
- We have included in our simulation geometry model, both the complex structure and material composition of the target (for target detail see **Figure 5**) of the cyclotron in order simulate with the highest detail the neutrons transport in the water volume inside the complex multi-material structure of the target itself.

2.2 Monte Carlo simulations of neutron transport

- The neutron spectrum around the cyclotron is not fully known. The most commonly used theoretical model to describe the source neutron spectrum that, is generated by the (p,n) nuclear reaction, is the evaporation model (Carrol, 1987, 2001, 2002; Bertini, 1963, 1965). The energy distribution of the emitted neutrons can be estimated by the expression $N(E)dE \propto E^{0.45} \exp(-E/\theta)$ where, θ is nuclear temperature, usually between 1 and 10 MeV. This expression has been selected as input for the energy distribution spectra for the isotropically-emitting neutron source in MCNP calculations, representing an evaporation model point-like neutron source (see **Figure 6**), with θ = 2.7 MeV (Carrol, 1987), located inside the water volume housed in the complex target structure (see **Figure 5**).
- The number of source neutrons, for each simulation run, was chosen to be 5.0 x 10^8 to have an MC statistical uncertainty less than 1% in each tally position.
- The three different F5 tallies point-detectors were positioned:
  - ✓ at 25 cm from the LV target externally to the cyclotron yoke surface,
  - ✓ at 100 cm from the target (near the outer wall surface in front of the LV target);
  - ✓ at 180 cm over the top of the cyclotron, vertically with respect to the center of the upper yoke surface.
- For each of three measurement positions (**LV, WALL** and **TOP**) the MCNP6-calculated spectra, reported in **Figure 7**, for that positions have been compared with SAND II outputs. Tally results, given as neutron fluence per neutron source particle, have been multiplied by the neutron source strength (3.345 x 10^{11} s^{-1}) to finally get, as output result, the differential neutron flux ($cm^{-2}s^{-1}MeV^{-1}$) to be used as guess spectrum for SAND II data processing.

FIG. 1

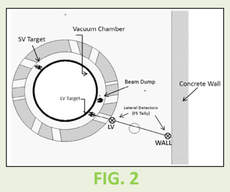

FIG. 2

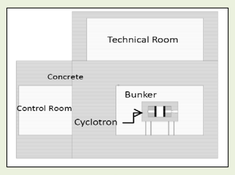

FIG. 3

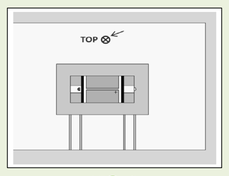

FIG. 4

The figures, 2, 3, 4 and 5 are obtained by the MCNP graphical user interface.

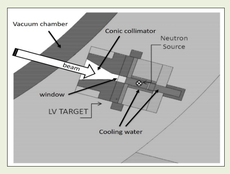

FIG. 5

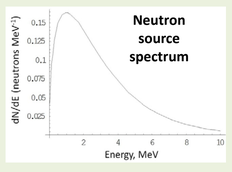

FIG. 6

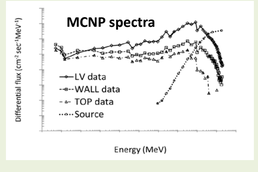

FIG. 7

3.Target foil irradiation and induced activity calculation

- In order to validate the Monte Carlo simulations, measurement of the neutron flux around the cyclotron with NAA (**Neutron Activation Analysis**) technique (Alfassi, 1994) has been performed and the experimental data have been processed with the SAND II code.
- In this work, three irradiation positions around the cyclotron, as indicated in **Figure 2**, have been selected as representatives of all the irradiation positions. In the case of neutron fields coming from a cyclotron, threshold reactions must be used to determine the fast flux component of the neutron spectrum coming from the nuclear reaction originating in the cyclotron target.
- The chosen set of foils can detect only the thermal and fast neutron flux components; to detect the epithermal component of neutron flux, the gold and copper foils have been also covered by a thin layer of cadmium which has a high thermal neutron capture cross section for, in this way, gold and copper foils mainly absorb the epithermal and fast components of the neutron flux.
- After the irradiation, at proton beam intensity of 30 μA for 60 minutes, the induced activity in each target foils was measured on a low-background HPGe detector (EG&G ORTEC).The multi-purpose gamma ray analysis software GammaVision® was used for peaks identification and evaluation. Details and data of the irradiated target foils are reported in **Table 1**.

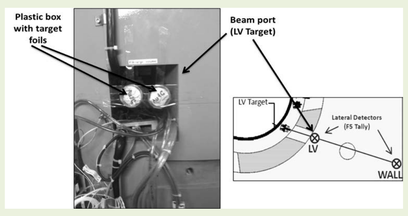

Left image: example of foils irradiation near the cyclotron LV target. Target foils have been placed in small plastic box and subjected to the same irradiation conditions. *Right image*: position of the lateral MCNP tallies (circle with cross symbols)

Element	Tl	Isotope %	Reaction	T_{count} (sec)	$t_{1/2}$	λ (sec^{-1})	E (keV)	A_{sat}
Au	^{197}Au	100	$^{197}Au(n,\gamma)^{198}Au$	$3.6x10^3$	2.69[d]	$2.971x10^{-6}$	411.79	$(3.945±0.197)x10^{-15}$
Au	^{197}Au	100	$^{197}Au(n,\gamma)^{198}Au(+)$	$3.6x10^3$	2.69[d]	$2.97x10^{-6}$	411.79	$(1.022±0.051)x10^{-15}$
Cu	^{63}Cu	69.1	$^{63}Cu(n,\gamma)^{64}Cu$	$3.6x10^3$	12.7[h]	$1.516x10^{-5}$	511	$(3.640±0.182)x10^{-14}$
Cu	^{63}Cu	69.1	$^{63}Cu(n,\gamma)^{64}Cu(+)$	$3.6x10^3$	12.7[h]	$1.516x10^{-5}$	511	$(5.221±0.261)x10^{-15}$
Fe	^{54}Fe	5.84	$^{54}Fe(n,p)^{54}Mn$	10^5	312.5[d]	$2.565x10^{-8}$	834.83	$(1.849±0.090)x10^{-15}$
Ni	^{58}Ni	68.1	$^{58}Ni(n,p)^{58}Co$	$6x10^4$	70.78[d]	$1.133x10^{-7}$	810.76	$(2.094±0.104)x10^{-14}$

Table1: Reactions used in this work for induced activities calculation. The symbol (+) beside reactions in the fourth column indicates foil irradiation with cadmium cover. (last column) errors correspond to one standard deviation of five repeated measurements on the detector.

4. Results

4.1 Data analysis, processing and iteration test controls

- The calculated values for target foils activity due to different nuclear reactions have been used as input data for the SAND II program which processes the different experimental data of the specific activity at saturation calculated starting from the measured induced activities in the target foils (for further details see Alloni et al., 2013). The final results of this comparison, are reported in the following Section (see **Figure 8**).

4.2 Comparison between simulation (MCNP) and experimental data (SAND II)

- **Figure 7** shows the MCNP-calculated neutron energy spectra plotted as a function of energy for 60 different energy groups, obtained with point detector tallies (F5 tally) in the three different position of interest labelled LV, WALL and TOP (see **Figure 2**). The calculated values of the total and thermal neutron fluxes in the same positions are also reported in **Table 2**. The thermal flux has been obtained summing the flux contributions in the first four energy bins corresponding to the energy range 0 - $6.9×10^{-7}$ MeV.
- Because of the scattering events, the spectra are shifted to lower energies with respect to the source term spectrum and the shift is larger at TOP and WALL position than LV, because neutrons undergo more collisions as the distance to the source (located in the target) increases. Furthermore, because the neutrons are strongly slowed down by the light materials of the walls, near the walls the spectrum is more thermalized.

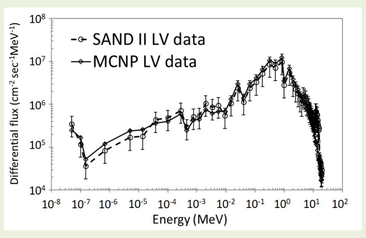

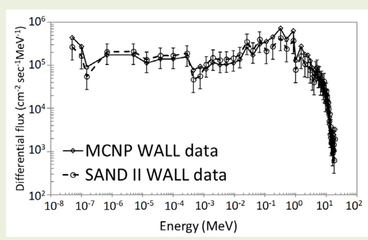

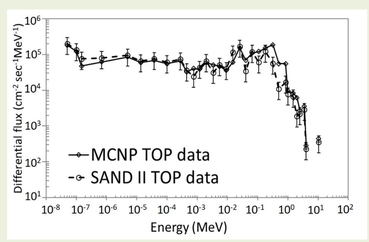

FIGURES 8: Comparison between the neutron flux spectrum obtained with MCNP6 simulations (continuous line with circles) and experimental data processed with the SAND II code (dotted line with square symbols) for different irradiation position. The errors for MCNP6 are limited to the symbols, error bars for SAND II data are reported.

Figures 7 show that measured and calculated spectra have the same behavior and are in good agreement. Moreover, the neutron spectra obtained in the site close to target position shows a peak in the high-energy region that is shifted to lower energies as the tally detector distance to the target increases where the contribution of epithermal and thermal neutrons became more effective.

Tally position	Total flux (cm^{-2} s^{-1})	Thermal flux (cm^{-2} s^{-1})
LV	$7.4973×10^7$	$4.9872×10^5$
WALL	$6.4102×10^6$	$5.1303×10^5$
TOP	$2.4485×10^6$	$8.1576×10^5$

Table 2: MCNP6 results for total and thermal flux in the three different positions around the cyclotron. For each reported value, Monte Carlo statistical standard (1σ) uncertainty is less than 1%.

4.3 Ambient dose estimation

- The calculated neutron spectra obtained wit MCNP6, considering the (ICRP 119, 2012) ambient dose equivalent-to-fluence conversion coefficients, were used to estimate the ambient dose equiva-lent H*(10). The calculated H*(10) in sites LV, WALL and TOP are reported in **Table 3**.
- The largest H*(10) value is observed in site WALL, while in the LV and TOP the H*(10) is lower due to neutron spectra modification (low energy shift) produced by the cyclotron body materials and the neutron scattering near the bunker concrete walls. Further experimental validation will be performed in future campaign.

Position	H*(10) (mSv/μAh)
LV	56 ± 0.4
WALL	84 ± 0.9
TOP	27 ± 0.5

Table 3: MCNP6-estimated values of H*(10), with Monte Carlo statistical standard (1σ) uncertainty, in different location around the cyclotron.

5. Conclusions

- In this work, we have characterized, with the MCNP6 Monte Carlo code, the secondary neutron flux spectra in three different locations around the cyclotron, using detailed cyclotron and target geometrical/composition computer models and compared the simulation results with experimental data obtained with NAA of thin target foils processed with SAND II code.
- The experimental data obtained in this work, are in good agreement with the MC simulations and these results represent a further validation the method proposed by the authors for a previous study and the characterization of the neutron field inside a subcritical assembly (Alloni et al., 2013) at the University of Pavia.
- The detailed reconstruction of the target geometry will allow a future study of the target dynamic under proton bombardment such as activation of the materials and dose depositions in different part of the target obtaining information useful for health physics program during maintenance of the machine for the most activated part.
- In this context, the method described in this work could represents a useful alternative to other methods described elsewhere, e.g. thermoluminescent method used in combination with Bonner sphere spectrometry (Mendez et al., 2002a, 2002b; Barquero et al., 2015)

REFERENCES

- Alfassi, Z.B., 1994. Chemical Analysis by Nuclear Methods. John Wiley and Sons, Inc..
- Alloni, D., Prata, M., 2017. Characterisation of secondary neutron field generated by a compact PET cyclotron with MCNP6 and experimental measurements, Applied Radiation and Isotopes 128 , 204-209
- Alloni, D., et al., 2013. Neutron flux characterization of the SM1 sub-critical multiplying complex of the Pavia University. Progr. Nucl. Energ. 67, 98-103.
- Barquero, R., Méndez, R., Vega-Carrillo, H.R., Iniguez, M.P., Edwards, T., 2005.Neutron spectra and dosimetric features around a 18 MV LINAC accelerator. Health Phys. 88, 48–58.
- Berg, S., McElroy, W.N., 1967. A computer-automated iterative method for neutron flux spectra determination by foil activation, Vol. II: SAND II (Spectrum Analysis by Neutron Detectors II) and Associated Codes, AFWL-TR-67-41.
- Bertini, H.W.,1963. Low energy intranuclear cascade calculations. Phys. Rev. 131 (4) 1801.
- Bertini, H.W.,1965. Low energy intranuclear cascade calculations. Phys. Rev. 138 AB2.
- Briesmeister, J.F., 2000. MCNP - A General Monte Carlo N-Particle Transport Code, Version 4C, Los Alamos National Laboratory report LA-13709-M.
- Carroll, L.R., 1987. Radiation measurements related to the design of a self-shielded accelerator system for routine use in PET. Proc. of the 34th Annu. Meeting of the Society of Nuclear Medicine, Vol 28.
- Carroll, L.R., 2001. Predicting long-lived induced activation of concrete in a cyclotron vault, AIP Conf. Proc. 576 301-4.
- Carroll, L.R., 2002. Estimating the radiation source term for PET isotope targets. 9th Int. Workshop on Targetry and Target Chemistry (Turku, Finland)
- Chadwick, M.B. et al., 2006. ENDF/B-VII.0: Next Generation Evaluated Nuclear Data Library for Nuclear Science and Technology. Nuclear Data Sheets, Special Issue on Evaluated Nuclear Data File ENDF/B-VII.0
- Goorley, T., 2012.Initial MCNP6 Release Overview, Nuclear Technology, 180, 298-315.
- Griffin, P.J., 1993. SNL RML Recommended dosimetry cross section compendium SAND92-0094.
- Griffin, P.J., 1994. User's Manual for SNL-SAND-II Code SAND-93-3957.
- IAEA TECDOC 1211, 2001. Charged particle cross-section database for medical radioisotope production: diagnostic radioisotopes and monitor reactions.
- IAEA TECHNICAL REPORTS SERIES No. 468, 2009.Cyclotron produced radionuclides: physical characteristics and production methods.
- ICRP 119, 2012. Compendium of dose coefficient based on ICRP publication 60. Annals of the ICRP, Vol 41, supplement 1.
- McElroy, W.N., Berg, S., Crockett, T., Hawkins, R.G. 1967. A Computer-Automated Iterative Method for Neutron Flux Spectra Determination by Foil Activation, Vol. I: A Study of the Iterative Method," AFWL-TR-67-41.
- Mendez, R., Iniguez, M.P., Barquero R., Mananes, A., Gallego, E., Lorente,A,.Voytchev, M., 2002a. Response components of LiF:Mg.Ti around a moderated ^{241}Am-Be neutron source. Radiat. Prot. Dosim. 98 173–8.
- Mendez, R., Barquero, R., Iniguez, M.P., Vega-Carrillo, H.R., Voytchev, M., 2002b.Thermoluminescence measurements of neutron dose around a medical linac. Radiat. Prot. Dosim. 101, 493–6.
- Williams III, R.G. , Gesh. C.J., Pagh, R.T., 2006. Compendium of Material Composition Data for Radiation Transport Modeling. Pacific northwest national laboratory - United States Department of Energy, PNNL-15870.